Egypt. J. Chem. **Vol. 67**, No. 1 pp. 167 - 179 (2024)

Egyptian Journal of Chemistry

http://ejchem.journals.ekb.eg/

"Anti-hepatic cancer, Antioxidant and Anti-inflammatory Effects of Palladium(II) Nano-Complex"

Safaa S. Hassan[a]*, Wafaa M Hosny[a]* and Perihan A. Khalf-Alla[a]

[a]*Department of Chemistry, Faculty of Science, Cairo University, Egypt*

Abstract

Cancer is a disease of the age and is a public name for a large group of diseases that can infect many parts of the body. One of the most deadly types is Hepatocellular carcinoma (HCC) which destroy one of the life-threatening organ (liver). The problem is cells of cancer tend to grow fast, chemo drugs can solve this problem by killing fast-growing cells and eliminating cancer. So, chemists are interested in the synthesis of new chemotherapeutic drugs. We synthesized new chemical compounds which are expected to be like chemotherapeutic drugs. The $[Pd(AEthP)Cl)]Cl.2H_2O$ was prepared in the nano and bulk size by the interaction between Pd(II) ion and 1-(2-aminoethyl) piperazine (AEthP) ligand. The particles were formed within 10-30 nm with square planar geometry. The separated drug was characterized by different analysis tools like; elemental analysis, Fourier transform infrared (FTIR), electronic spectra, magnetic measurement and molar conductance techniques. The nano-size was confirmed by using the scanning electron microscope (SEM) technique. The optimized geometrical parameters were calculated. The formation constants of binary and ternary complexes were calculated, these complexes were formed due to the interaction between the synthesized drug with some selected bio-molecules. The most predominant species in the physiological range (pH of blood) between the synthesized drug with the selected bio-molecules were determined by plotting the speciation diagrams. It was found that the hepatocellular cytotoxic activity of the suggested drug within the bulk size was inactive, but its cytotoxic activity was observed (IC_{50} equals 20 µg/mL) by decreasing its size to the nano-scale. The same observation was noticed in the case of antibacterial activity. The docking active site interactions were evaluated using the selected proteins, Cyclin-dependent kinases (CDKs) (anticancer activity) and protein crystal structure of GlcN-O-P synthase (antimicrobial activity). It was observed that the aqua-form $[Pd(AEthP)OH_2)]^{2+}$ of the synthesized drug had powerful antioxidant and anti-inflammation activity in comparison to both its chloro-form $[Pd(AEthP)Cl)]^{+}$ and the standard common drugs.

Keywords: 1-(2-aminoethyl) piperazine, nano-size; antioxidant, anti-inflammation; HEPG2; stability constant; concentration distribution diagram.

1. Introduction

Cancer of the liver is increasing globally [**1,2**]. Primary liver cancer is the sixth most prevalent cancer worldwide and the fourth primary cause of cancer-related mortality [**3**]. In 2018, for instance, liver cancer affected 841,000 persons and caused 782,000 fatalities worldwide. Inflammation, a part of the body's defense system, is an additional risky condition. It is the process by which the immune system recognizes and eliminates detrimental and foreign stimuli; nevertheless, chronic inflammatory diseases (stroke, chronic respiratory diseases, heart disorders, cancer, obesity, and diabetes) [**4,5**] are the leading cause of mortality worldwide. Chronic diseases are, according to the World Health Organization (WHO), the greatest hazard to human health [**6**]. There are many side effects associated with anti-inflammatory drugs. Therefore, the solution is the synthesis of novel chemotherapeutic medicines. In the last decades, nano-dimensional materials (1–100 nm size) can be produced and applied in a number of technological and consumer fields because of their peculiar physicochemical properties [1]. Metallic-based nano compounds have attracted much scientific attention particularly, nano-sized noble metal materials which have important and valuable uses for the benefits potentially offered in a number

*Corresponding author e-mail: hsafaa@sci.cu.edu.eg

Receive Date: 14 April 2023, Revise Date: 13 May 2023, Accept Date: 01 July 2023

DOI: 10.21608/EJCHEM.2023.206084.7870

of different applications. Palladium nanoparticles have attracted researchers because of their great potential in medical science as well as clinical therapy [2]. Many new Pd (II) complexes especially with different amine ligands having favorable anticancer activity against tumor cell lines with minimum side effects have been synthesized and reported [3-10]. Also, scientists reported that a complex of Pd nanoparticles demonstrated highly effective antitumor and antimicrobial activity than bulky palladium complexes [11]. In fact, palladium complexes of nucleobases and their derivatives become of current interest because they form faster than their platinum analogs and produce analogous products in solution [12,13]. In biological fluids, millions of potential ligands are likely to compete for metal ions in *vivo* [14]. So, mixed-ligand complexes play a key role in biological chemistry [15-22] and have been extensively studied. The mode of bonding and structure of these and related ligands have been exhaustively studied potentiometrically by the evaluation of the mixed ligand stability constants. They have been shown to be monodentate via the N_3 of the pyrimidine and N_7 of the purine bio-ligands as shown in Figure 1. The attack of reactive species like free radicals on body cells causes damage and tumor formation. Therefore, Metal-based antioxidants have received recent scientific attention for their capacity to protect organisms and cells from damage induced by oxidative stress [23-26]. Trapping the free radicals was used to measure the antioxidant activity of the synthetic compounds [27]. Inflammation is the body's natural protective response to tissue injury caused by physical or chemical stimuli or invading microbial toxins. Prolonged inflammation can lead to chronic inflammatory diseases such as asthma, rheumatoid arthritis, multiple sclerosis, Parkinson's and Alzheimer's diseases and cancer [28-33]. There are many side-effects associated with anti-inflammatory drugs. Hence, it's necessary to discover novel anti-inflammatory compounds with higher efficiency and lower side effect. So, our study is an attempt to get a novel Palladium (II) triamine drug with high antibacterial, antioxidant, cytotoxicity and anti-inflammation properties. Also, the equilibrium interaction with biorelevant will be investigated and finally the molecular docking interactions with the selected proteins will be discussed.

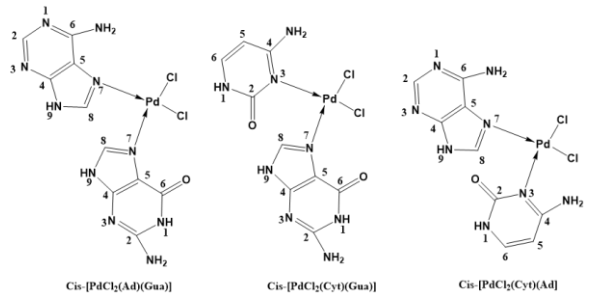

Fig. 1. Proposed structures of some Palladium(II) mixed ligand complexes.

2. Experimental

2.1. Materials and reagents

All reagents used were of analytical grade and of the highest purity. They included $PdCl_2$(B3333940), 1-(2-aminoethyl)piperazine(AEthP)(A55209), alanine(A7627), glycine(G8898), inosine(I4125), inosine monophosphate(57510), uracil(26088), uridine(SA46201), imidazole(I2399), methylamine(65572), KH_2PO_4(P0662), sodium hydroxide(567530), $AgNO_3$(209139) and ethyl alcohol(E7148). All these reagents were provided from Aldrich and Sigma Chemical Co. Whatman Filter Paper Grade 5 and cytiva whatman aqueous IFD 0.2micrm.

2.2. Preparation (Pd-AEthP) complex (in bulk and nano size)

Nanostructure Pd(II) complex was prepared by heating $PdCl_2$ (1.0 mmol) and KCl (0.149 g; 2.0 mmol) in the least amount of water to 70^{o}C with stirring. The clear solution of $[PdCl_4]^{2-}$solution was cooled to 25 ^{o}C, filtered and gradually poured into (during 20 min) an ethanolic solution of AEthP (1 mmol in 20 mL) under ultrasonic irradiation. After complete addition, the resulting reaction mixture was kept in the ultrasonic bath for a period of 60 min. But the bulk precipitate was formed by refluxing 2 hrs. Green and yellow precipitates were filtered and dried under vacuum for nano and bulk complexes respectively.

2.3. Instruments

Potentiometric measurements were performed using a Metrohm 686 microprocessor equipped with a 665 Dosimat (Switzerland-Heri-sau). The temperature was maintained constant inside the cell at 25.0 ± 0.1 ℃, by the circulating water by a thermostated bath [34,35].

Elemental microanalysis of the separated solid chelates for Carbon, Hydrogen and Nitrogen was

performed by standard microanalysis methods using Automatic analyzer CHNS Vario EL III-Elementar, Germany at Microanalytical Center, Cairo University, Giza, Egypt.

FT-IR spectra were obtained with the KBr disc technique using a test scan Shimadzu FTIR spectrometer. The spectra were collected in the range 250-4000 cm^{-1}.

^{1}H-NMR spectra were recorded using 300 MHz Varian-Oxford in DMSO-d_6 as a solvent and the chemical shifts were recorded in ppm relative to TMS as an internal standard.

Electronic absorption spectra in DMF were measured using automated UV/Vis-NIR 3101 PC Shimadzu spectrophotometer ranged from 200-900 nm.

The molar magnetic susceptibility was measured using the Faraday method on powdered samples. The diamagnetic corrections were made by Pascal's constant and $Hg[Co(SCN)_4]$ was used as the calibrant.

Molar conductivity of metal complexes was measured for 1.00 x 10^{-3} M DMSO solutions at 25 ± 1ºC using the conductivity meter ORION model 150 of 0.6 cell constant.

2.4. Procedure of potentiometric titrations

At First, $[Pd(AEthP)Cl]^+$ was converted into aqua form by treating it with one equivalent $AgNO_3$, and stirring overnight (with careful protection from light) as described elsewhere [36]. The precipitate was filtered out and the resulting yellow filtrate was used directly. Then, the acid dissociation constants of the bio-ligands were determined by titrating 0.05 mmol samples of each with standard NaOH solution. Also, the acid dissociation constants of the coordinated water molecule in $[Pd(AEthP)H_2O]^{2+}$ were determined by titrating 0.05 mmol of this complex against 0.05M NaOH solution. Finally, the formation constants of this aqua complex with bio-relevant ligands were determined by titrating a solution mixture of 0.05 mmol of $[Pd(AEthP)H_2O]^{2+}$ and bio-relevant ligand with a ratio 1:1(Pd:L). The calculations were carried out using the program MINIQUAD-75 [37]. Also, the concentration distribution curves were obtained with the SPECIES program [38].

2.5. Molecular orbital calculations (DFT calculation)

Through this section, we try to examine the optimized geometrical parameters (bond lengths and bond angles), net charges on active centers and energy of the ground state for (AEthP) ligand and its complex with Pd(II) ion. In all calculations, Density Functional Theory (DFT) is used at the B3LYP level [39], 3-21G as a basis set for the ligand [40] and LANL2DZ as basis set for (Pd-AEthP) complex [41]. All calculations proceeded using G09W program [42].

2.6. Antimicrobial assay

The antimicrobial activities of (AEthP) and its Pd(II) complex for both bulk and nano sizes were investigated using the agar well diffusion method [43,44]. All the compounds were tested *in vitro* for their antibacterial activity against *staphylococcus aureus* and *Streptococcus mutans* (Gram positive bacteria), *Pseudomonas aeruginosa* and *klebsiella*(Gram negative bacteria) using nutrient agar medium. Ampicillin and Gentamicin were used as standard drugs for Gram-positive and negative respectively. all of these tests were carried out at 15 mg/mL concentration (stock solution of tested compounds). Nutrient agar was prepared and then poured into Petri-dishes and allowed each petri-dish to cool down to room temperature. The tested compounds were dissolved in DMSO, which was used as solvent control as it has no inhibition activity with different concentrations. A circular well was made at the center of each petri-dish with a sterilized steel borer. Then, 100 µL of each test solution was added to the well using a micropipette and the plate was incubated; 24 h for bacteria and 48 h for fungi at 37℃ then the diameter of the inhibition zone was reported. This experiment was carried out in triplicate and zones of inhibition were measured in mm scale. The standard deviation was calculated. Also, the fold change of the nano-complex relative to the bulk was mentioned = (Result value (nano-complex) / Result value(Bulk complex)

2.7. Antitumor measurements

Evaluation of the cytotoxic activity of Pd(II) complex for both bulk and nano sizes was carried out in *vitro* using the Sulfo-Rhodamine-B-stain(SRB)[45,46]. SRB is a protein stain to provide a sensitive index of cellular protein content. The Cells were seeded in 96-well Microtiter plates at an initial concentration of $3x10^3$ cell/well in a 150 µl fresh medium and left for 24 hours to attach to the plates. Five different concentrations 0, 5, 12.5, 25, 50 µg/mL of the drug were added. For each drug concentration, 3 wells were used for each individual dose. The plates were incubated for 48 hours. The cells were fixed with 50 µl cold trichloroacetic acid 10% final concentration for 1 hour at 4 ^{0}C. (Automatic washer Tecan, Germany) with distilled water were used to wash the plates. 50 µl 0.4 % SRB dissolved in 1 % acetic acid was used to stain the plates at room temperature for 30 minutes. Each well was measured at 570 nm spectrophotometrically using an ELISA microplate reader (Sunrise Tecan reader, Germany). The mean value of the background absorbance was

automatically subtracted and of drug concentration was calculated. Three times is the repetition of each experiment. The cell survival percent was calculated by: Surviving fraction = optical density (O. D.) (Treated cells) / O. D. (Control cells). Also, the IC_{50} values (the concentrations of tested compounds required to produce 50% inhibition of cell growth) were calculated. Doxorubicin was used as a standard liver antitumor drug. The IC_{50} fold change of the nano-complex relative to the bulk was mentioned = (Result value (nano-complex) / Result value(Bulk complex)

2.8. Antioxidant activity

In *vitro* antioxidant activity, test samples were allowed to react with 1,1-diphenyl-2-picrylhydrazyl radical for half an hour at 37°C. Various concentrations of test samples were incubated with DPPH. After incubation, the decreasing in absorption was measured at 517 nm. Percentage radical scavenging activity (% RSA) achieved by samples was determined, in comparison with DMSO treated control group. The standard deviation was calculated.

2.9. Denaturation inhibition measurements of bovine serum albumin

Test solution containing different concentrations of the drug was mixed with albumin solution in phosphate buffer and incubated at 27°±1°C in a BOD incubator. Denaturation was achieved by keeping the reaction mixture at 60°±1°C. The percentage of inhibition of denaturation was calculated. Each experiment was done in triplicate and the average was taken.

3. Results and discussion

3.1. Solution section

The acid dissociation constants of AEthP ligand were determined under experimental conditions of 25°C and using $NaNO_3$ to adjust ionic strength at a constant of 0.1 mol dm^{-3} which were also used for determining the stability constants of the Pd(II) complexes. The results obtained are in good agreement with the literature data [47].

Acid-base equilibria of $[Pd(AEthP)(H_2O)]^{2+}$

The best-fit model for the potentiometric data of $[Pd(AEthP)(H_2O)]^{2+}$ was found to be consistent with two species: 10-1 and 20-1. (10-1)species is due to deprotonation of the coordinated water molecule, as represented in Eq.(1). The dimeric-μ-hydroxo complex, 20-1, is formed due to the interaction between 100 and 10-1 species according to Eq.(2) [48

$$\underset{100}{[Pd(AEthP)(H_2O)]^{2+}} \overset{Ka_1}{\rightleftharpoons} \underset{10\text{-}1}{[Pd(AEthP)(OH)]^{+}} + H^{+}, \quad \text{Eq.(1)}$$

$$[Pd(AEthP)(OH)]^{+} + [Pd(AEthP)(H_2O)]^{2+} + H_2O \rightleftharpoons \underset{20\text{-}1}{[Pd(AEthP)(OH)(AEthP)]^{3+}}, \quad \text{Eq.(2)}$$

pK_a value for $[Pd(AEthP)(H_2O)]^{2+}$ is 6.40. The equilibrium constant of the dimerization was calculated using the relationship: $\log K_{dimer} = \log \beta_{20\text{-}1} - \log \beta_{10\text{-}1} = 3.84$.

The species distribution diagram for $[Pd(AEthP)(H_2O)]^{2+}$ and its hydrolyzed species was shown in Figure 2. The dimeric species, 20-1, predominates between pH 4.2–6.8 with a maximum concentration of 51% at pH 6.4. The monohydroxy species, 10-1, is the main species above pH ~ 6.4. This reveals that the predominant species present under the physiological pH range, i.e., pH 6-7 is 10-1 and 20-1 which can interact with DNA constituents.

Complex-formation equilibria of ternary mixed ligand complexes with bio-molecules

The best-fitted model for the potentiometric data of Pd(AEthP)-glycine as a representative example of amino acid was found to be consistent with the unprotonated form 110. The value of $\log \beta_{110}$ (5.90) for this ternary complex was found to be less than those of $[Pd(N\text{-}N)(H_2O)]^{2+}$, $\log \beta_{110} \approx 10–12$ [49-52]. The high stability value is due to the diamine complexes having two available sites for coordination. So, amino acid coordination can occur through both the carboxylate oxygen and the amino group forming a more stable mixed ligand chelate with five-membered ring. However, in the case of $[Pd(AEthP)(H_2O)]^{2+}$, it had one site only available for coordination so amino acids may coordinate through the amino group or the carboxylate oxygen. Initially, at low pH, the coordination is carried out through the carboxylate oxygen when the amino group is protonated. But with increasing the pH, the coordination site is changed to the amino group that is more favored for Pd atoms. In the case of

imidazole and methylamine, both of them coordinate through amino group forming unprotonated species 110. ($\log\beta_{110}$) of methylamine is higher than that of imidazole. This may be due to the highest basicity of the amino group of methylamine as reflected by its highest pK_a value. All these results are listed in **Table 1**. DNA constituents act as monodentate ligand and form 1:1 complexes with $[Pd(AEthP)(H_2O)]^{2+}$. However, inosine-5′-monophosphate forms the mono-protonated complex 111 and the di-protonated species 112, in addition to the formation of 110 species. The pyrimidine bases as uracil and uridine have basic nitrogen donor atoms (N_3) [53,54] in the measurable pH range, and they form 1:1 species with $[Pd(AEthP)(H_2O)]^{2+}$.As a result of the high pK_a values of pyrimidines (pK_a> 9), the ternary complexes are formed completely only above pH ~ 6, confirming that the negatively charged nitrogen donor of these ligands is important binding site in the physiological pH range (blood pH). Therefore N-donor ligands have affinity for $[Pd(AEthP)(H_2O)]^{2+}$, which may have important biological implications because the interaction with DNA is thought to be responsible for the antitumor activity of related complex. Concentration distribution diagram of inosine as a representative example, **Figure 3**, shows the formation of the species 110 at low pH and predominate in the physiological pH range with maximum formation degree of 76%. The monohydroxy species 11-1 has no contribution.

Table 1. Formation constants for mixed ligand complexes of $[Pd(AEthP)(H_2O)]^{2+}$ with bio--ligands at 25 °C and 0.1 mol dm^{-3} ionic strength.

System	M L H^a	logβb	System	M L H^a	logβb
Pd(DME)-OH	1 0 -1 2 0 -1	-6.40(0.01) -2.56(0.03)	**Inosine**	0 1 1 1 1 0	8.43(0.01) 7.00(0.06)
Glycine	0 1 1 1 1 0	9.76(0.01) 5.90(0.10)	**Inosine monophosphate**	0 1 1 0 1 2 0 1 3 1 1 0 1 1 1 1 1 2	8.95(0.01) 15.27(0.01) 17.10(0.07) 7.50(0.09) 16.33(0.05) 23.27(0.05)
Imidazole	0 1 1 1 1 0	7.04(0.01) 4.96(0.10)			
Methylamine	0 1 1 1 1 0	10.03(0.01) 6.99(0.07)	**Uracil**	0 1 1 1 1 0	9.28(0.01) 12.98(0.08)
$H_2PO_4^{2-}$	0 1 1 1 1 0 1 1 1	-7.20(0.01) 3.62(0.06) 8.299(0.04)	**Uridine**	0 1 1 1 1 0	9.01(0.01) 9.08(0.10)

M, L and H are the stoichiometric coefficients corresponding to pd(AEthP),ligand and H^+, respectively.; the coefficient −1, refers to a proton loss.

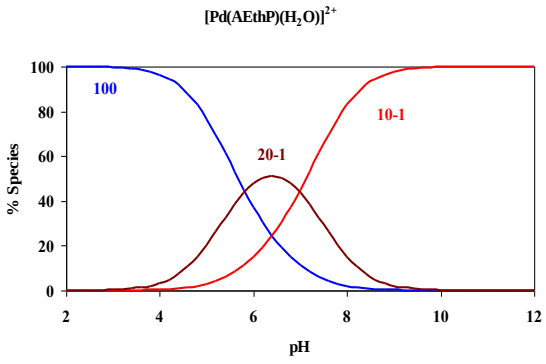

Fig. 2. Concentration distribution of various species as a function of pH in the [Pd(AEthP)-H_2O]$^{2+}$ system.

3.2. Solid section

Investigation of palladium(II) complex

One new complex of Pd (II) with 1-(2-aminoethyl) piperazine (AEthP) with empirical formula $[Pd(AEthP)Cl)]Cl.2H_2O$.

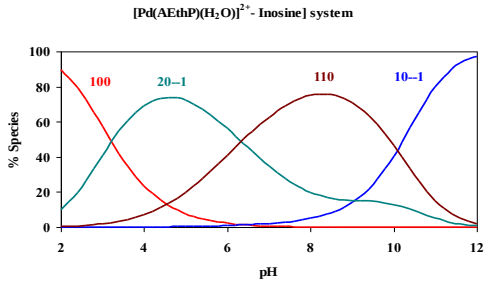

Fig. 3. Concentration distribution of various species as a function of pH in the $[Pd(AEthP)(H_2O)]^{2+}$with inosine.

The elemental analysis for metal complex shows a satisfied agreement between the experimental (C: 20.60, H: 5.33 and N: 12.0) and theoretical results (C: 21.04, H: 5.59 and N: 12.27). The stoichiometric ratio of the synthesized complex is 1:1 (M:L). The complex was prepared in the nano-size as represented using scanning electron microscope in **Figure 4**.

The characteristic infrared spectral data observed and vibration assignments of ligand (AEthP) and its palladium complex are reported in **Table 2**. The spectrum of the ligand supports the existence of ν(N-H) which belonged to primary and secondary amine groups in addition to $\upsilon(C\text{-}H)_{aliphatic}$ and $\upsilon(CH_2)$ modes. The stretching frequency of (NH) group of (Pd-AEthP) complex was shifted towards lower frequency indicating the coordination of the nitrogen atom to Pd(II) ion [55,56]. Also, the spectra of solid complex exhibited a broad band in the region 3200-3500 cm^{-1} were assigned to the ν(OH) of water **[**57**].** There is overlapping between absorption band of ν(OH) and $\nu(NH_2)$ as both of them located at 3441cm^{-1}. New band was observed in the far-IR region for this complex around 525-620 cm^{-1}corresponding to υ(M–N) bands [58]. Another new band was found in the region 290–350 cm^{-1} for (Pd-AEthP) chelate is due to υ(M-Cl) [59]. So, from the results of IR spectral, we concluded that AEthP ligand behaves as a tridentate ligand through three nitrogen atoms of amine groups.

The^{1}H-NMR spectra of AEthP and its diamagnetic Pd(II) complex recorded in DMSO-d_6 using tetramethylsilane (TMS) as internal standard. From The^{1}H- NMR spectra of AEthP complex, we noticed that there is no appreciable change in the position of both piperazine ring and aliphatic group protons where it is in the same range as observed in the spectra of AEthP(ligand). The position of signals corresponding to $–NH_2$ and –NH group protons changed in the (Pd-AEthP) complex where it is shifted to low field side from (8.20 to 7.93) ppm and (4.80 to 3.71) ppm respectively indicating that the nitrogen atoms are coordinated to the metal ion [60,61]. Moreover, new signal that observed at 3.34 ppm(s,4H) is assigned to protons of water molecules held in the lattice [62].

On the basis of the conductivity, values below 50 $Ω^{-1}$ $ohm^{-1}cm^2$ in DMSO solution are non-electrolytes [63,64]. So, (Pd-AEthP) complex has electrolytic nature, the molar conductance is considered as a test to know the degree of ionization of the prepared complexes. If the anions (chloride ion) are present outside the coordination sphere, the molar conductivity of the investigated complex will be significant. Then, we can assume that the prepared complex has one chloride ion outside the coordination sphere. It indicates that the ionic nature of this complex 1:1 (electrolyte) [65,66]

The UV-VIS spectra show an absorption band for (AEthP) as a ligand at 350nm assigned to n-π* charge transfer transition [67]. $[Pd(AEthP)Cl]Cl.2H_2O$ is diamagnetic as expected for square planar d^8systems. The electronic spectra display two bands at 603 and 389 nm due to $^1A_{1g} \rightarrow {}^1B_{1g}$ and L-MCT. So, these results prove the square planar geometry around Pd(II) **[**68,69]. All the absorption bands were fully assigned in **Table 2**.

According to all previous data, the proposed structure can be shown in **Figure 5**.

Fig. 4. SEM for nano structure Pd(II)-AEthP complex (10-30 nm).

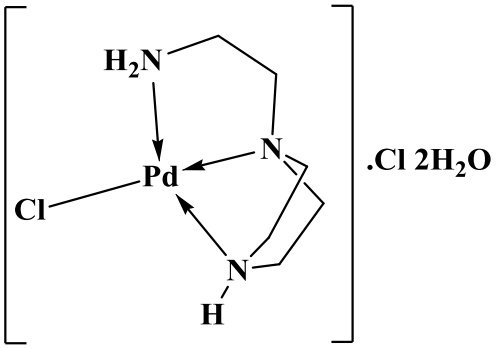

Fig. 5.The suggested structure of Pd complex.

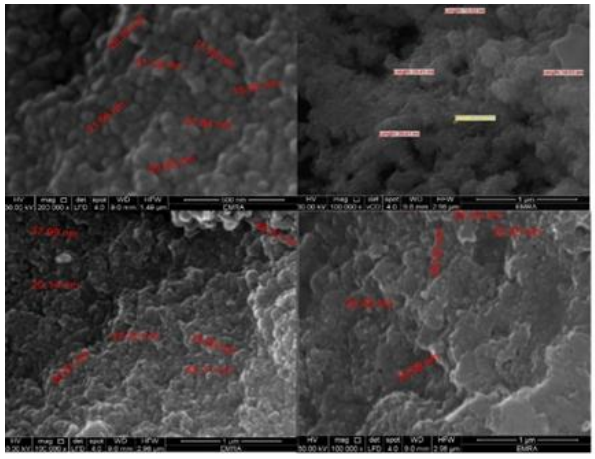

Table 2. IR frequencies, electronic absorption bands and magnetic moments of [AEthP] ligand and its Pd(II) complex (4000- 250cm^{-1}).

	AEthP	**[Pd(AEthP)Cl]Cl.2H$_2$O**
υ(NH$_2$),(OH)water	3356	3441overlapping
υ(NH)	3282	3205
υ(C-H)aliphatic	2943	2951
υ(CH$_2$)	1462	1454
υ(M-N)	---	501, 551
υ(M-Cl)	---	331
λ_{max} (nm)	350	603 389
Assigned Transition	n-π* Charge Transfer	$^1A_{1g} \rightarrow {}^1B_{1g}$ L-MCT
B.M.	---	Diamagnetic

3.3. *Structure characterization with DFT study*

The geometric structures of AEthP ligand and Pd (II)-AEthP complex were optimized as shown in **Figure 6**.

Upon coordination of the three (N) atoms to the Pd atom, N-C types bond lengths become slightly longer than in the free ligand accompanied with changes in angles that were clarified in **Table 3** producing distorted square planar geometry.

The formal charge of palladium was +2 but the calculated natural population charge on the palladium complex was 0.027. It can be explained due to the strong σ-donor of AEthP ligand.

The molecular properties are mentioned in **Table 4** which can be calculated as follows: Hardness η = (I-A)/2, Softness (S) S= 1/ 2η, Chemical potential (μ), μ = -(I +A)/2 Electronegativity (χ), χ = (I + A)/2 and Electrophilicity index (ω), ω = μ^2/2η.

HOMO and LUMO molecular orbital energy diagrams are presented in **Figure 6**. From HOMO-LUMO gap (ΔE), one can detect whether the molecule is hard or soft. Larger ΔE corresponding to harder molecule and small one related to the softer molecule. The polarizability of the soft molecule is more than the hard one because it needs lower energy to excitation, thus Softness (S) and hardness (η) are properties of molecule that measures the chemical reactivity.

Table 3. Some of the optimized bond lengths, Å and bond angles, degrees, for AEthP ligand using B3LYP/6-311G(++)d,p and their Pd(II) and Pt (II) complexes using B3LYP/LANL2DZ.

Bond length (A^o)	**AEthP**	**Pd- AEthP**	**Bond angles (Deg.)**	**AEthP**	**Pd- AEthP**
R(N1-C2)	1.470	1.492	**A(C6-N1-C7)**	115.249	115.066
R(N1-C6)	1.467	1.492	**A(N1-C6-C5)**	113.566	109.258
R(N1-C7)	1.466	1.487	**A(N1-C7-C8)**	111.916	112.704
R(C3-N4)	1.469	1.569	**A(C2-C3-N4)**	113.226	108.437
R(N4-C5)	1.469	1.479	**A(C3-N4-C5)**	111.510	112.055
R(C8-N9)	1.468	1.484	**A(N4-C5-C6)**	112.778	108.450
R(N4-M)	---	2.437	**A(C7-C8-N9)**	110.022	111.317
R(N9-M)	---	2.322	**A(N4-M-N9)**	---	144.643
R(M-Cl)	---	2.461	**A(N4-M-Cl)**	---	113.148
Bond angles (Deg.)	AEthP	Pd- AEthP	**A(N1-M-N9)**	---	80.488
A(C2-N1-C6)	110.350	109.433	**A(N1-M-Cl)**	---	177.505
A(C2-N1-C7)	114.426	114.908	**A(N9-M-Cl)**	---	101.304
A(N1-C2-C3)	34.199	109.304			

Table 4. Ground state properties of AEthP ligand using B3LYP/6-31G(++)d,p and its Pd(II) complex using B3LYP/LANL2DZ.

Parameter	AEthP	Pd- AethP	Parameter	AEthP	Pd- AEthP
E_T, Hartree	-402.0121	-543.5925	**χ, eV**	2.66	0.73
E_{HOMO}, eV	-5.26	-3.92	**η, eV**	2.59	2.14
E_{LUMO}, eV	-0.069	0.37	**S, eV^{-1}**	0.38	0.46
ΔE, eV	5.191	4.29	**M, eV**	-2.66	1.77
I=- E_{HOMO}, eV	5.26	3.92	**Ω, eV**	1.36	0.73
A= - E_{LUMO}, eV	0.069	-0.37	**Dipole Moment (Debye)**	1.6882	11.4173

3.4. Microbiological and cytotoxic activity with docking investigation

The antibacterial study was performed using the different gram-positive and gram-negative bacteria as mentioned in **Table 5**. The inhibition zones revealed that the ligand had much antibacterial effect than the bulk and nano-Pd(II) complex. From **Table 4**, the dipole moment of the ligand is much lower than the Pd complex that illustrates the difference in the antibacterial activity because the polarity can be indicated by the dipole moment property. As the dipole moment value of the tested compound decreases as the lipsolubility increases then penetrates the lipid layer of the microorganism and destroys it more effectively [70].

Fig. 6. Optimized geometries of AEthP and Pd-AEthP compounds with their Molecular graphs.

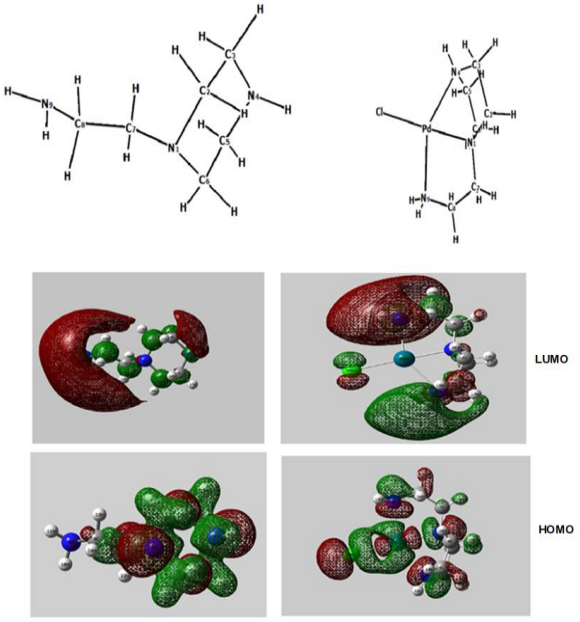

It was shown in **Figure 7** shows that the biological activity of Pd-AEthP complex in the nanoscale against all types of microorganisms was improved than the complex in the bulk scale. This nano size is more suitable in penetration and interaction with the microorganisms. The previous improvement was achieved also with the cytotoxic activity using the human hepatocellular carcinoma cell line (HepG-2) as represented in **Figure 8**. The bulk Pd complex is considered to be inactive against HepG-2 while with the decrease in its size to the nanoscale, its activity starts to be observed with IC_{50} = 20 µg/mL as seen in **Table 5**. The binding affinity of AEthP and its Pd complex against GlcN-O-P synthase receptor (PDB ID: 1XFF) was investigated because GlcN-6-P synthase may be exploited as a target for potential antibacterial drug, since it is an important life-sustaining enzyme present in all kinds of bacterial cells [71]. It represents the possible interaction between the tested compounds and the active amino acids of GlcN-O-P synthase receptor. **Figure 9(1)** shows arene-cation interactions between the NH and NH_2 function groups of the suggested drug with the active Trp74 amino acid.

In the case of cytotoxic molecular docking study, Cyclin dependent kinases (CDKs) are considered a potential target for anti-cancer medication. The cell will die by interfering the drug with CDK action. The interaction was carried out with Asp-145 as was observed in **Figure 9(2)**

3.5. DPPH radical scavenging assay

The activity of antioxidants on DPPH radical is believed to be centered on their ability to donate hydrogen [72]. DPPH become a stable molecule after the acceptance of hydrogen radical or an electron [73]. In our study, the interaction of the suggested drug with DPPH radical leads to the decrease in DPPH absorbance at 517 by the action of hydrogen

Complex name	**IC_{50} (µg/ml)**
Pd-AEthP (Bulk)	Not achieved
Pd- AEthP (Nano)	20 (Nano)
Doxorubicin	4.58
Fold change of the nano-complex relative to the bulk	---

Table 5. Half-maximal inhibitory concentration (IC_{50} (µg/ml)) values against (HepG2 Hepatocellular cancer)

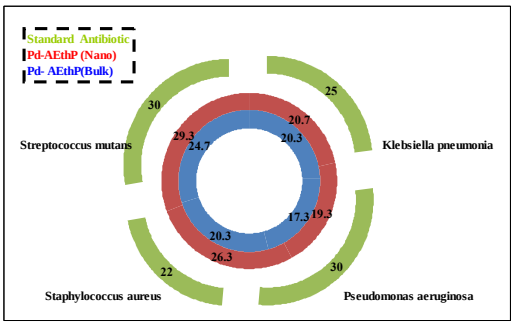

Fig. 7. Biological activity of AEthP, Pd-AEthP(Bulk) and Pd- AEthP (Nano), towards different types of bacterial strains.

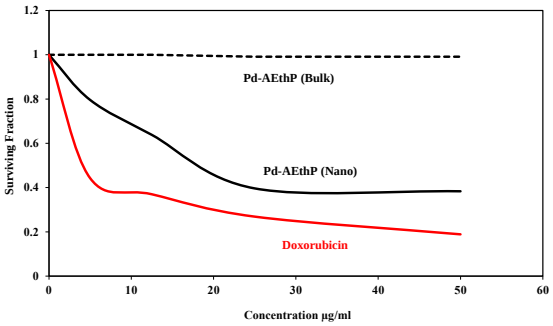

Fig. 8. The surviving fraction (HepG2 Hepatocellular cancer) with the concentration change of the suggested Pd(II) complex in the bulk and nanoscale.

donation mechanism **Scheme 1**. The antioxidant activities of the tested compounds were arranged as Pd(AEthP)-OH_2>Pd(AEthP) >AEthP according to IC_{50} value and radical activity percentage **Figure 10**. The high antioxidant activity of the equated form of the complex was in comparable to the standard vitamin C may be explained due to the proton dissociation of water molecule (10-1) species become more acidic upon complexation with Pd(II) ion **Table 1**.Its dissociation constant value is near to the standard (Vit. C) ($pKa_1 \approx 4$) [74] depending on the hydrogen donation principle [72] as discussed above and pointed out in (**Scheme 1**). Furthermore, the binuclear formation probability (20-1) increases the antioxidant activity by its lower ionization constant as mentioned before in the solution section.

Species diagram **Figure 1** confirmed that 20-1 species are the most predominant species at the physiological pH. Also, the results showed the lower activity of the free ligand (< 50%) which may due to its higher proton dissociation constants then the difficulty of scavenging the free radical [75].

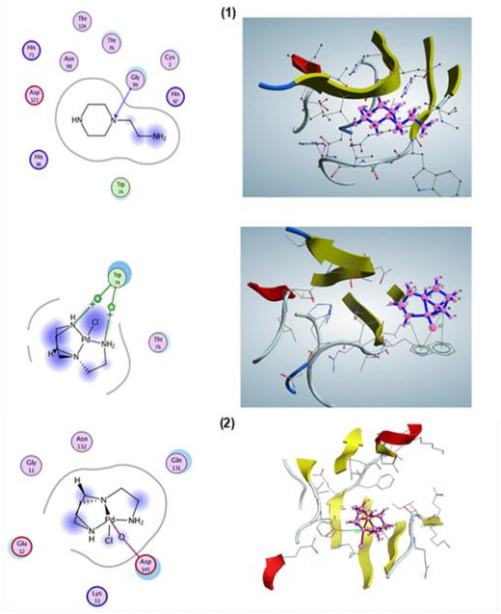

Fig. 9.(1) Interactions of AEthP and Pd-AEthP on the active sites of GlcN-O-P synthase receptor (PDB ID: 1XFF) (2) Interactions of Pd-AEthP on the active sites of Cyclin dependent kinases (CDKs) (PDB ID: 1FVV)

3.1. In-vitro anti-inflammatory activity

The different forms of the synthesized complex were screened for anti-inflammatory activity by using the inhibition of albumin denaturation technique. From the results of anti-inflammatory activity, we can notice that the aqua form Pd(AEthP)-OH_2 showed maximum activity when compared to Ibuprofen standard drug and the chloro form Pd-AEthP-Cl. This is due to the more labile water molecule making easier interaction with albumin protein and causing inhibition for its denaturation.

Also, the aqua form of the complex has the highest positive charge that enhances the attraction to the negatively charged BSA molecule at pH 7 [76]. Comparing the ligand and complexes, it was found that the presence of metal ions in the case of complexes increases the binding affinity with the albumin skeleton that allows the denaturation inhibition effect, while the free ligand depends on hydrogen bond formation only as seen in Figures 11.

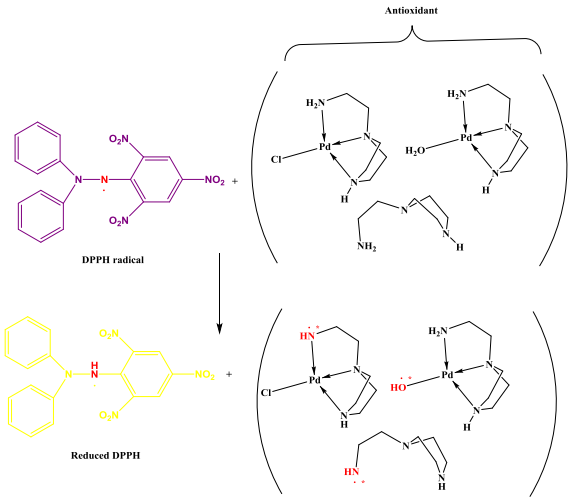

Scheme 1. Conversion of DPPH*(purple) to its corresponding hydrazine form (yellow) by the addition of AEthP, Pd- AEthP-Cl and Pd(AEthP)-OH2 compounds to DPPH* due to proton transfer.

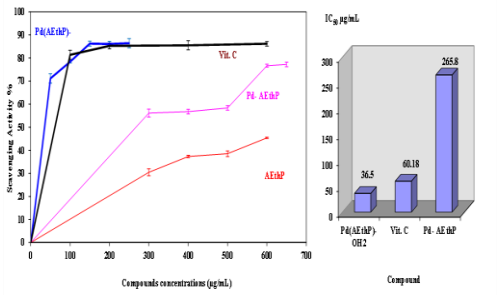

Fig. 10. DPPH scavenging potential and IC50 of AEthP, Pd-AEthP-Cl and Pd(AEthP)-OH_2.

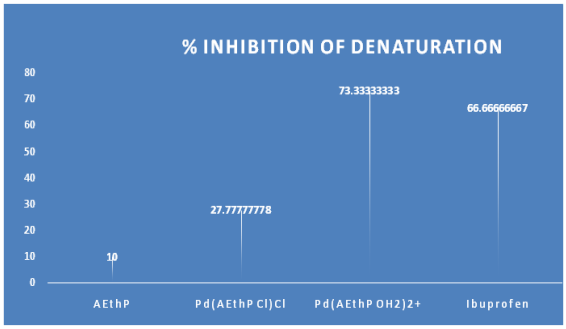

Fig. 11. In *vitro* anti-inflammatory of all complex forms.

Table 6. Antibacterial activity data of the synthesized Pd(II) complex, inhibition zone (mm).

Sample	Inhibition zone diameter (mm/mg sample)			
	Bacteria			
	Klebsiella pneumonia (ATCC:4415)(G⁻)	***Pseudomonas aeruginosa (ATCC:27853)(G⁻)***	***Staphylococcus aureus (ATCC:6538)(G⁺)***	***Streptococcus mutans (ATCC:25175) (G⁺)***
Standard Antibiotic	**Gentamicin**		**Ampicillin**	
	25 ± 0.5	30 ± 0.5	22 ± 0.1	30 ± 0.5
AEthP	39.7 ± 0.6	30± 0.6	48.3 ± 0.7	30 ± 1.0
Pd-AEthP (Bulk)	20.3 ± 0.6	17.3 ± 0.5	20.3 ± 0.6	24.7 ± 0.6
Pd- AEthP (Nano)	20.7 ± 0.6	19.3 ± 0.5	26.3 ± 0.6	29.3 ± 0.5
Fold change of the nano-complex relative to the bulk	1.019	1.115	1.295	1.186

4. Conclusions

In this work Pd(II) complex with 1-(2-aminoethyl) piperazine (AEthP) in nano-size was synthesized and characterized. The analytical and physicochemical data confirmed the composition and structure of the newly obtained compound. (AEthP) ligand behaved as tridentate ligand by using three nitrogen atoms with 1:1 (metal: ligand) stoichiometry with square planar geometry. (Pd-AEth) complex in bulky scale showed lacked of activity against growth human liver cancer HepG2 and this activity became to increase in nano-size complex with IC_{50}= 20 µg/mL. Moreover, both ligand and its complex showed antibacterial activity but (AEthP) parent ligand had much antibacterial effect than the bulk and nano Pd(II) complex. The docking active sites interactions were evaluated. In addition to the antioxidant and inflammatory activities were studied and the aqueous form of the synthesized palladium complex has the maximum activity.

5. Conflicts of interest

"There are no conflicts to declare".

6. References

1- M.Arnold,C.C.Abnet,R.E.Neale,J.Vignat,E.L.Giovannucci,K.A.McGlynn,etel.,Gastroenterlogy,2020,159,335.
2- Y.E.Chon,S.Y.Park,H.P.Hong,D.Son,J.Lee,E.Yoon,et al.,Clin Mol Hepatol.,2023,29,120.
3- Y.E.Chon,S.W.Jeong,D.W.June, Clin Mol Hepatol.,2021,27,512.
4- E. Elinav, R.Nowarski, C. A.Thaiss, B. Hu, C. Jin and R. A.Flavell.*Nat. Rev. Cancer,* 2013**,** 13, 759-771.
5- J. L. Pablos and J. D. Canete. Curr. Top. Med. Chem., 2013, **13**, 705–711.
6- S. G. Dos, V. K. utuzov and K. M. Ridge. *Mol. Physiol.*, 2012**, 303**, 627–633
7- O. V. Salata, J Nanobiotech., 2004, **2**(1),3.
8- Y. Yoshihisa, A. Honda,Q.L. Zhao , T.Makino andR. Abe et al. ExpDermatol., 2010, **19**, 1000–1006.
9- J. R. Benson, I. Jatoi, M. Keisch, F. J. Esteva, A. Makris, and V. C. Jordan,Lancet., 2009**, 373**(9673), 1463–1479.
10- M. Galanski, Recent Patents on Anti-Cancer Drug Discovery, 2006**, 1**(2), 285–295.
11- S. S. Hassan, S. M. Gomha, *Chem. Pap*. **2019**, 73, 331
12- S. S Hassan, D. H Hanna, S. S Medany, *Appl. Organomet. Chem*. **2023**, 37, 1-19
13- S. S. Hassan, P. A. Khalf-Alla, *Appl. Organomet. Chem*. **2020**, 34, 1.
14- V. F. Lotfy, S. S. Hassan, P. A. Khalf-Alla, A. H. Basta, *Int J Polym Mater*, **2020**, 69, 21-31
15- S. S. Hassan, E. A. Bedir, A. El-Rahman M. Hamza, A. M. Ahmed, N. M. Ibrahim, M. S. Abd El-Ghany, N. N. Khattab, B. M. Emeira, M. M. Salama, E. F. Mohamed, D. B. Fayed, *Appl. Organomet. Chem.,* **2022**, 36, 1-19.
16- S. S. Hassan, R. N. Shallan, MM Salama, Journal of Organomet. Chem. 911, 121115
17- A. F. El-Husseiny and H. H. Hassan, SpectrochimActa A Mol. Biomol. Spectrosc., 2013, 103, 232–245.
18- C. Navarro-Ranninger, E. I. Montero, I. L´opez-Solera, J. R. Masaguer, and B. Lippert, J. Organomet. Chem., 1998**, 558**, 103–110.
19- A. S. Abu-Surrah, K. A. Abu Safieh and I. M. Ahmad et al., Eur. J. Med. Chem., 2010**, 45**(2),471–475.

20- A. S. Mildvan and M. Cohn, J. Biol. Chem., 1966, **241**(5), 1178–1193.
21- G. M. R. Tombo and D. Bellus,Angew. Chem., 1991**, 103**(10), 1219–1241.
22- E F Mohamed and S S Hassan, Egypt. J. Chem., 2022, **65**(12), 11–19.
23- M Shoukry, S Hassan, Open Chemistry 2012 (3), 318-324
24- M. M. Shoukry, A. A. Shoukry, P. A. Khalf Alla, S. S. Hassan, *Int. J. Chem. Kinet.,* **2010**, 42, 608-618
25- MM Shoukry, SS Hassan, Spectrochimica Acta Part A: Molecular and Biomolecular Spectroscopy 118, 146-153
26- SS Hassan, MM Shoukry, AAQ Jbarah, Journal of the Mexican Chemical Society 64 (2), 97-116
27- PA Khalf-Alla, AH Basta, VF Lotfy, SS Hassan, Macromolecular Materials and Engineering 306 (3), 2000633
28- A Al-Alousi, PA Khalf-Alla, SS Hassan, MM Shoukry, Journal: Journal of Advances in Chemistry 9 (3)
29- A. A. Al-Amiery, A. A. H. Kadhum, and A. B. Mohammed, BioinorgChem Appl., **2012**, 6 (2012).
30- PA Khalf-Alla, SS Hassan, MM Shoukry, Inorganica Chimica Acta 492, 192-197
31- S. S. Hassan, E. Fares Mohamed, *Appl. Organomet. Chem*. **2019**, 34, 1-11
32- S. A. Aly, S. S. Hassan, A. S. Eldourghamy, E. E. Badr, M. A. El-Salamoney, M. A. Hassan, *Appl. Organomet. Chem*. **2022**, 36, 1.
33- A. Choudhary, R. Sharma, M. Nagar, M. Mohsin, and H. S. Meena, J ChilChem Soc., 2011, **56**(4),911–917.
34- SS Hassan, MM Shoukry, RN Shallan, R Van Eldik, J. of Coord. Chem. 70 (10), 1761-1775
35- SS Hassan, MM Shoukry, R van Eldik, Dalton Transactions 41 (43), 13447-13453
36- M. R. Shehata, M. M. Shoukry, F. M. Nasr and R. van Eldic, Dalton Trans., 2008**, 779**.
37- P. Gans, A. Sabarini and A.Vacca, InorgChimActa, 1976, **18**,237.
38- L. Pettit. Personal Communication, University of Leeds, 1993.
39- A. D. Becke. J. Chem.Phys., 1993**, 98(7)**, 5648–5652.
40- M. P. McGrath and C. Radom. J. Chem. Phys., 1991**, 94**, 511-516.
41- P. J. Hay and W. R. Wadt. J. Chem. Phys., 1985**, 82**, 299-310.
42- M. J. Frisch and G.W. Trucks, et al.. Gaussian, Inc., Wallingford CT(2009).
43- M. S. A. El-Gaby. J. Chin.Chem. Soc., 2004**, 51**, 125-134.
44- A. C. Scott. Laboratory control of antimicrobial therapy. In: Collee JG et al. eds. Practical Medical Microbiology, 13th Edition. Edinburgh: Churchill Livingstone, 1989**, 161**.
45- V. Vichai and K. Kirtikara. Sulforhodamine B colorimetric assay for cytotoxicity screening, 2006, **179**.
46- H. Alshater, A. I. Al-Sulami, S. A. Aly, E. M. Abdalla, M. A. Sakr, S. S. Hassan, Molecules **2023**, 28, 2590.
47- A. Kiss, E. Farkas, I. Sóvágó, B. Thormann and B. Lippert.J. Inorg. Biochem., 1997**, 68** (2), 85-92.
48- Z. Nagy, I. Sóvágó. *J. Chem. Soc., Dalton Transactions*, 2001**, 17**, 2467–2475.
49- M. R. Shehata. Trans. Met. Chem., 2001**, 26** (1–2), 198-204.
50- M. R. Shehata, M. M. Shoukry, F. M. Nasr and R. van Eldik. Dalton Trans., 2008, **6**,779-786.
51- M. R. Shehata, M. M. Shoukry, F. H. Abdel-Shakour and R. van Eldik.Eur. J. Inorg. Chem., 2009, **26**, 3912-3920.
52- M. R. Shehata, M. M. Shoukry, A. A. Osman and A. T. AbedelKarim. Spectrochim. Acta A, 2011**, 79** (5), 1226-1233.
53- H. Sigel, S. S. Massoud and N. Acorfu.J Am Chem Soc.,**116**, 959(1994).
54- MM Shoukry, SS Hassan, The Scientific World Journal 2013
55- S. J. swamy and B. K. Kumar, Indian J. Chem., 1996, **35A**, 489-493.
56- S. J. Swamy, B. VeeraPratap, P. Someshwar, K. Suresh and D. Nagaraju, J. Chem. Res., 2005, 313-315.
57- G.Xue, Z.Juenfong, G.Shin, Y. Wu and B.Shuen, J. Chem. Soc Perkin Trans. **II**, 1989, 33.
58- K. H. Schmidt, A. Muller. Coord. Chem. Rev., 1976, **19**,41-97.
59- M. Y. Ali, T. Baraki, R. K. Upadhyayand A. Masood. Am. J. Appl. Chem., 2014, **2**, 15-18.
60- S. J. Swamy, P. Someshwar,Spectrochimi.Acta Part A, 2008, **70**, 929-933.
61- S. Chandra,L. K. Gupta and Sangeethika,Spectrochim. Acta A., 2005**, 62**,453-460.
62- W. H. Mahmoud, G. G. Mohamed and M. M. I. El-Dessouky. Int. J. Electrochem. Sci., 2014, **9**, 1415.
63- W. J. Geary, Coord. Chem. Rev., **7**, 81(1971).
64- L.K. Thompson, F.L. Leeand E.J. Gabe, Inorg. Chem. 1988, **27**, 39.
65- P. Skehan and R. Storeng. J. Natl. Cancer Inst., 1990, **42**, 1107.

66- W.M.I. Hassan, M.A. Badawy, G.G. Mohamed, H. Moustafa and S. Elramly. Spectrochim. Acta A, 2013**, 111** , 169.
67- C. K. Jorgensen. Absorption Spectra and Chemical Bonding in Complexes. Pergamon Press, London(1964).
68- S. I. Mostafa,Transit Metal Chem., 2007**, 32(6)**,769–775.
69- S. I. Mostafa, M. M. Bekheit. Chem. Pharm. Bull., **48(2)**,266–271(2000).
70- M. Carcelli, P. Mazza, C. Pelizzi, G. Pelizzi and F. Zani, J. Inorg. Biochem., 1995, 57, 43.
71- W. Marek, M. Slawomir, M. Jan and B. Edward, ActaBiochim. Pol., 2005, 52, 647.
72- I. P. Ejidike and P. A. Ajibade, J. Coord. Chem., 2015, 68, 2552–2564.
73- I. Gülçin, Ö. I. Küfrevioglu, M. Oktay, and M. E. Büyükokuroglu, J Ethnopharmacol., 2004, 90, 205–215.
74- E. P. Serjeant and B. Dempsey, Pergamon, Oxford, 1979.
75- R. E. Reichard and W. C. Fernelius, J. Phy Chem., 1961**, 65**, 380.
76- D. Fologea, B. Ledden, D. S. McNabb and J. Li, ApplPhysLett., 2007, **91**(5), 053901(1)-053901(3).